Fault Modeling and Estimation for CMG

Qiang Shen, Xiang Yu, and Chengfei Yue

Abstract— **Momentum exchange devices like reaction wheel (RW) and control moment gyro (CMG) are always used as actuators in spacecraft attitude control systems. However, the unexpected faults in these momentum exchange devices may result in mission failures or even the spacecraft breakup. To enhance the reliability and safety of the attitude control systems, this paper addressed the CMG fault modeling and estimation problems in attitude control systems. We model the CMG as a combination of two EM-VSD (electrical motor (EM) and variable speed drive (VSD)) systems. All potential faults in an EM and a VSD are analyzed and mathematically modeled. Based on the fault model of a EM-VSD system, the CMG fault model consisting of faults in two EM-VSD systems are developed. An observer based fault estimation method is then proposed, in which the past gimbal angle and commanded gimbal rate are utilized to estimate the total CMG fault effects. It is proved that the gimbal and fault estimation errors converge to small compact sets containing origin. To verify the proposed fault estimation method, numerical simulations are carried out based on a model of a rigid spacecraft.**

I. Introduction

In practical space missions, redundant momentum exchange devices are equipped in spacecraft to enhance the reliability, maneuverability and survivability [1], [2], [3]. For spacecraft attitude control systems, this redundancy makes the spacecraft an over-actuated system and provides a larger momentum envelope than three conventional control effectors in attitude maneuver. However, if a fault occurs in the momentum exchange devices, the output torques acting on the spacecraft may be different from the commands from the attitude controller. For instance, the TOPEX satellite cannot perform attitude maneuvers due to the failure of pitch reaction wheel, which leads to the mission failure in October 2005 [4]. Recently, the Mars Odyssey (launched in 2001) came into the protective standby mode in 2014 due to the failure of a reaction wheel. How to avoid the failure of the space mission and the economic losses caused by the actuator faults has become an important matter in the field of spacecraft control.

Due to the advantages of simple structure and high torque amplification capability, single gimbal control moment gyro (SGCMG) is frequently used as actuators in agile spacecraft, which requires fast attitude maneuver and high pointing precision. It is noted from the mechanical structure that the SGCMG can be considered as an integration of a gimbal control system and a wheel speed control system. Comparing to RW that changes the magnitude of angular momentum while its direction is fixed, SGCMG is a constant-speed rotor mounted on a gimbal frame such that the direction of angular momentum keeps changing but its magnitude is a constant. Since either gimbal control loop or the wheel speed control loop can be modeled as an electrical motor (EM) with its variable speed drive (VSD) system, SGCMG is regarded as a combination of two EM-VSD systems. All potential faults can occur in the mechanical part of the EM, sensors and actuators of VSD, and the electrical part of these components.

To enhance the system reliability and prevent the control performance deterioration after the occurrence of actuator fault or failure in spacecraft missions, various fault tolerant control strategies have been developed [5], [6], [7], [8], [9], [10], [11], [12]. In [5], the mechanism of RW faults is analyzed but the mathematical fault model is not given explicitly. In [9], a mathematical model accounting for four different kinds of RW faults is developed. Based on this fault model, a finite-time fault-tolerant controller is designed to compensate the RW fault effects for a rigid spacecraft subject to saturation constraints. In [7], the skew angle of a pyramid CMG configuration is tuned through a genetic algorithm to handle CMG failures. In [11], the sliding mode control approach is adapted to change the CMG gimbal rate directly to void the singularity and deal with CMG faults. However, the mechanism of CMG is not clearly addressed and the general CMG fault model is not established in [11].

In this paper, the SGCMG is considered as a combination of two EM-VSD systems, which can govern the gimbal angle control loop and wheel speed control loop. Each EM-VSD system governs one degree of control freedom and works independently. Based on this structure and considering the potential faults in EM-VSD system, a general fault model for SGCMG is established with a clear understanding of mechanical mechanism. Specifically, a fault occurring in an EM-VSD system is modeled as a multiplicative fault or an additive fault according to how it affects the SGCMG output, and the resulting SGCMG fault model is in a generally applicable form of cascade multiplication of two EM-VSD systems. Then, we develop an adaptive observer to estimate the total fault effects in gimbal control loop. The total impact of SGCMG faults is estimated instead of each fault itself, which reduces the complexity and time in fault estimation, especially when several kinds of fault occur concurrently. In addition, it is also convenient for

Q. Shen is with Department of Mechanical and Aerospace Engineering, the School for Engineering of Matter, Transport and Energy, Arizona State University, Tempe, AZ, USA. Email: qiang.shen@hotmail.com

X. Yu is with the School of Automation Science and Electrical Engineering, Beihang Univerisity, Beijing, People's Republic of China. Email: xiangyu1110@gmail.com

C. Yue is with the Department of Electrical and Computer Engineering, National University of Singapore, Singapore 119077. Email: chengfei_yue@u.nus.eduu

designing the reconfigurable controller via the estimated total fault effects as they can be compensated in a similar way to external disturbances. Finally, the effectiveness of the proposed SGCMG fault estimation method is demonstrated through numerical simulation.

The remaining parts of this paper are organized as follows. Section II presents the mathematical model of an EM-VSD system and a SGCMG. Section III presents the proposed fault estimation approach. In Section IV, numerical simulation in a rigid spacecraft using four SGCMGs as actuators is carried to verify the proposed fault estimation method. Finally, this paper ends with the conclusion in Section V.

II. SGCMG Fault Model

A SGCMG consists of a constant-speed rotor mounted on a gimbal frame, and this mechanical structure can be essentially modeled as a cascade combination of two EM-VSD systems, which describe the dynamics of the rotor control loop and gimbal frame control loop, respectively. It is obvious that each EM-VSD system controls one degree of freedom and works independently. In this section, we first establish the fault model for the EM-VSD system and then apply it to the SGCMG to achieve the SGCMG fault model.

A. Fault Model of a EM-VSD System

The details about potential faults in an EM-VSD system are analyzed in [13], [14], [15], [16]. For the EM, potential faults are categorized into [15]:

- bearing faults;
- the stator or mature faults;
- the broken rotor bar and end ring faults of induction machines and
- the eccentricity-related faults.

With regard to the VSD, the faults are classified into:

- mechanical and electrical faults;
- actuator faults (actuator in the VSD) and
- sensors faults.

Generally speaking, it is noted that mechanical faults (faulty bearings, brush wear, shaft misalignment, eccentric rotor, etc.) and electrical faults (broken rotor bars, windings short-circuit, etc.) are due to mechanical wearing, harsh working environment, aging and severe voltage stresses. These faults belong to the multiplicative faults, which can be represented by the control gain change. In addition, the motor fault in VSD would cause the situation that the power device is not able to provide sufficient voltages or currents to drive the EM. As a result, the related sensor cannot characterize the physical phenomenon properly in the event of faults. These faults are considered as the additive faults [16], [17], which have effects similar to measurement bias or external disturbances.

The schematic diagram of the EM-VSD system considering potential faults is shown in Fig. 1, where the red lines represent the essential physical connection of the system, the black line represents the potential measurement of the input or output of actuators, $u(t)$ is the commanded control

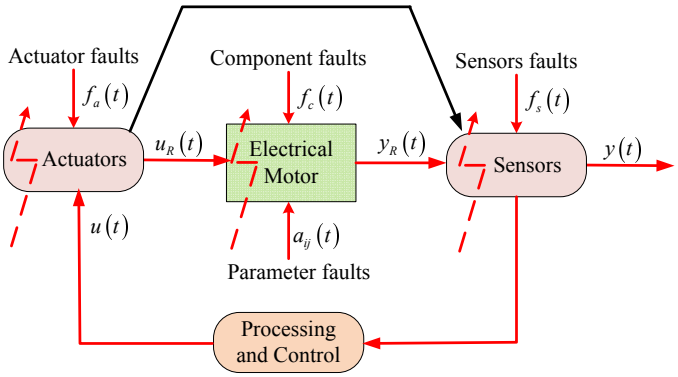

Fig. 1. Fault model of EM-VSD system

input from controller, $u_R(t)$ denotes the actual or real output control action, $y_R(t)$ denotes the actual or real states, $y_(t)$ denotes the state measurements, and $f_a(t)$, $f_c(t)$, $f_s(t)$, and $a_{ij}(t)$ are EM-VSD actuator faults, component faults, sensor faults, and parameter faults, respectively.

Based on our previous work in [18], the general fault frame of an EM-VSD system is given by

$$\begin{cases} \omega = \eta_\omega \omega_c + \omega_a, & \text{Speed control loop} \\ \dot{\delta} = \eta_\delta \dot{\delta}_c + \dot{\delta}_a, & \text{Gimbal rate control loop} \end{cases} \tag{1}$$

where ω and ω_c are rotating speed of the flywheel and its command input, $\dot{\delta}$ and $\dot{\delta}_c$ are gimbal rate and its command from CMG steering law, η_ω and η_δ are effectiveness gains of speed and control torque, ω_a and $\dot{\delta}_a$ are offsets of angular velocity and control torque.

B. SGCMG Fault Model

As shown in Fig. 2, a SGCMG contains a spinning rotor mounted on a gimbal. In the nominal condition, the rotor is required to hold a constant speed and the gimbal is manipulated to change the direction of angular momentum. As a result, a gyroscopic reaction torque that is orthogonal to both the rotor spin direction and gimbal axis is generated. With a small input torque to the gimbal, a larger control torque is produced to act on the spacecraft. This is the so-called torque amplification characteristic. Specifically, the torque generated by a CMG is proportional to the plane spanned by the angular momentum vector and gimbal angular rate vector, which can be thereby computed as:

$$\tau = -h_0 \dot{\delta}_c \hat{t}, \tag{2}$$

where h_0 denotes the constant angular momentum of the spinning rotor since the rotor has a constant speed, and $\hat{t}$ denotes a unit vector in the direction of output torque. The negative sign " - " in (2) implies the output torque lies in the opposite direction of $\hat{t}$.

The potential faults in a SGCMG may be from rotor speed control loop and/or the gimbal angle control loop. For a SGCMG, we consider the rotor loop as the first degree of freedom and the control loop of gimbal frame as the second degree of freedom. Here, we assume that the rotor control system and the gimbal control system work

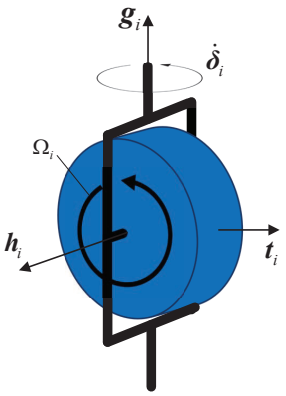

Fig. 2. Schematic of a SGCMG

independently. That is to say, the dynamics of rotor and gimbal will not influence each other in its own dynamics. For the rotor control system, which can be modeled as an EM-VSD system, the angular momentum is the product of its inertia and the rotor angular velocity, i.e. $h_0 = J\omega$. With consideration of the possible fault in EM-VSD, the rotor momentum is described as:

$$h_{f0} = J(\eta_\omega \omega_c) + h_a, \tag{3}$$

where $h_a = J\omega_a$ is the momentum offset.

In light of (1), the fault model of gimbal loop can be expressed as:

$$\dot{\delta}_f = \eta_\delta \dot{\delta}_c + \dot{\delta}_a. \tag{4}$$

Replacing h_0 and $\dot{\delta}_c$ by h_{f0} and $\dot{\delta}_f$ in (2), the output torque generated by SGCMG subject to faults is given by

$$\tau_f = -(J\eta_\omega \omega_c + h_a)\left(\eta_\delta \dot{\delta}_c + \dot{\delta}_a\right)\hat{t}. \tag{5}$$

To this end, we build the SGCMG fault model considering potential faults in both rotor control loop and gimbal control loop. Noting that the SGCMG saturation is not considered as a fault since it's a kind of constraint. It is clear that different combination of coefficients η_ω, h_a, η_δ, and $\dot{\delta}_a$ may represent different fault situation and SGCMG working conditions. In the following, the nominal work condition is denoted as N, which is regarded as a benchmark output. Then in each single loop (either gimbal control loop or rotor control loop), its working condition is defined as:

- N : Nominal working condition;
- F_a : Partially lose effect, without offset;
- F_b : Completely fail, without offset;
- F_c : Partially lose effect and have offset and
- F_d : Totally fail and have offset.

In summary, the fault modes of SGCMG under different situations are shown in Table I.

TABLE I

WORKING CONDITIONS AND FAULT MODELS OF SGCMG

Rotor	Gimbal	Model
N	N	$-h_0\dot{\delta}_c\hat{t}$
	F_a	$-h_0\eta_\delta\dot{\delta}_c\hat{t}$
	F_b	0
	F_c	$-h_0\left(\eta_\delta\dot{\delta}_c+\dot{\delta}_a\right)\hat{t}$
	F_d	$-h_0\dot{\delta}_a\hat{t}$
F_a	N	$-J\eta_\omega\omega_c\dot{\delta}_c\hat{t}$
	F_a	$-J\eta_\omega\omega_c\eta_\delta\dot{\delta}_c\hat{t}$
	F_b	0
	F_c	$-J\eta_\omega\omega_c\left(\eta_\delta\dot{\delta}_c+\dot{\delta}_a\right)\hat{t}$
	F_d	$-J\eta_\omega\omega_c\dot{\delta}_a\hat{t}$
F_b	N,F_a,F_b F_c,F_d	0
F_c	N	$-(J\eta_\omega\omega_c+h_a)\dot{\delta}_c\hat{t}$
	F_a	$-(J\eta_\omega\omega_c+h_a)\eta\dot{\delta}_c\hat{t}$
	F_b	0
	F_c	$-(J\eta_\omega\omega_c+h_a)\left(\eta_\delta\dot{\delta}_c+\dot{\delta}_a\right)\hat{t}$
	F_d	$-(J\eta_\omega\omega_c+h_a)\dot{\delta}_a\hat{t}$
F_d	N	$-h_a\dot{\delta}_c\hat{t}$
	F_a	$-h_a\eta_\delta\dot{\delta}_c\hat{t}$
	F_b	0
	F_c	$-h_a\left(\eta_\delta\dot{\delta}_c+\dot{\delta}_a\right)\hat{t}$
	F_d	$-h_a\dot{\delta}_a\hat{t}$

III. FAULT ESTIMATION FOR SGCMG

In the previous Section, we consider SGCMG as a cascade combination of two EM-VSD systems and develop fault models for gimbal control loop and rotor control loop, respectively. In this Section, we propose a fault estimation scheme for SGCMG gimbal control loop to estimate potential gimbal fault. In practical mission, multiple SGCMGs are employed to generate the commanded torques from controller. Here, we assume that N SGCMGs are equipped in the spacecraft, and each of N SGCMGs may occur faults. To obtain the fault information in each SGCMG, we develop local fault estimator for each SGCMG. The overall attitude control system with local fault estimate is demonstrated in Fig. 3.

As for each SGCMG, the rotor rotates at a constant speed. If a fault occurs in the rotor, the undesired rotor speed can be recognized easily by rotational speed measurement. Therefore, the rotor fault is not considered in this Section and we only design estimator to gimbal fault. Recalling (4), the gimbal fault in SGCMG is modeled as

$$\dot{\delta}(t) = \eta_\delta \dot{\delta}_c(t) + \dot{\delta}_a, \tag{6}$$

where η_δ is a constant denoting the control effectiveness gain, $\dot{\delta}_a$ denotes the additive bias fault or offset which is also a constant, $\dot{\delta}_c$ is the commanded gimbal rate from CMG steering law, and $\dot{\delta}$ is the actual output rate.

To reduce the notation burden in the following fault estimate design, let $r_c(t) = \dot{\delta}_c(t)$, $e = \eta_\delta$, and $r_a = \dot{\delta}_a$. As a consequence, the gimbal fault model in (6) is rewritten as

$$\dot{\delta}(t) = e r_c(t) + r_a. \tag{7}$$

In practice, it is easy to measure the gimbal angle that will be used as a measurement for gimbal fault estimation.

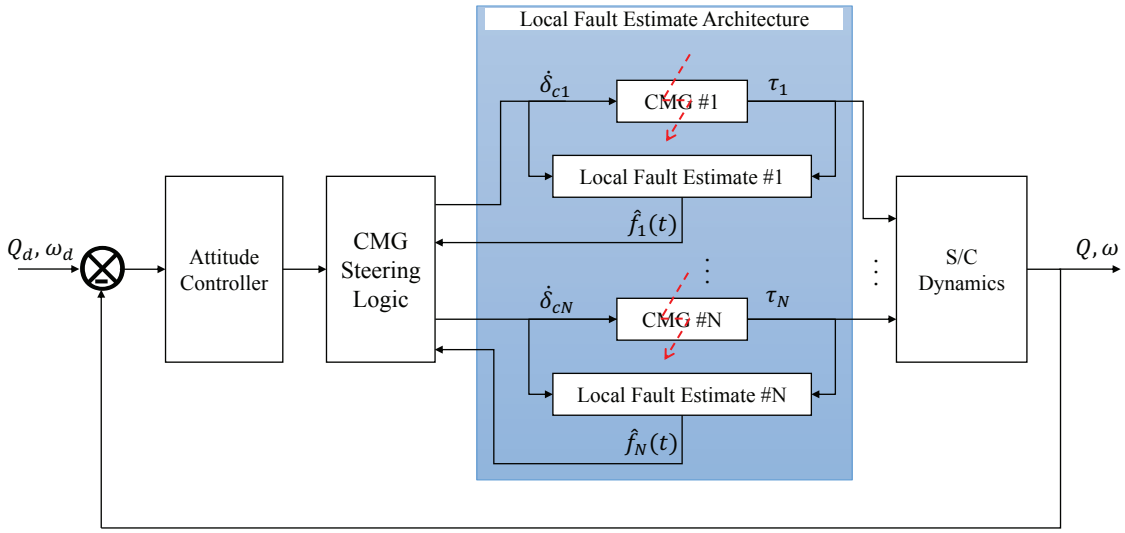

Fig. 3. Overall attitude control system with local fault estimation

A. *Fault Estimation*

For each SGCMG, the gimbal fault model in (7) is further written as

$$\dot{\delta}(t) = r_c(t) + f(t). \tag{8}$$

where $f(t) = (e-1)r_c(t) + r_a$ represents the total fault effect lumping the loss of effectiveness fault and additive bias. Due to the physical limitation of the SGCMG, the commanded gimbal rate $r_c(t)$ and the additive bias fault r_a are bounded. In addition, since e is the actuator effectiveness which varies between 0 and 1 in practice, it is obtained that the magnitude of the total fault effects $f(t)$ is bounded as $|f(t)| \le f_a$, where f_a is a positive constant.

In the proposed fault estimation approach, we will estimate this total fault effects $f(t)$ in each SGCMG rather than each individual fault itself. That is, we do not estimate e and r_a separately, and only estimate the total fault effect represented by $f(t)$. If we proceed to estimate individual actuator fault, the fault estimation approach may be complicated and time-consuming, especially when several kinds of fault occur concurrently in the system. Besides a simple design structure in fault estimation scheme, it is also convenient for designing the reconfigurable controller via the estimated total fault effects as they can be compensated in a similar way to external disturbances.

Next, an adaptive observer for the fault estimation is proposed as follows:

$$\dot{\hat{\delta}}(t) = r_c(t) + l_1[\delta(t) - \hat{\delta}(t)] + \hat{f}(t) \tag{9}$$

$$\hat{f}(t) = k\hat{f}(t-T) + l_2[\delta(t) - \hat{\delta}(t)] \tag{10}$$

where T is the updating interval, l_1, l_2, and k are positive design parameters chosen by the designer. Define estimation errors $\tilde{\delta}(t) = \delta(t) - \hat{\delta}(t)$ and $\tilde{f}(t) = f(t) - \hat{f}(t)$. Then the estimation error dynamics is given by

$$\dot{\tilde{\delta}}(t) = -l_1\tilde{\delta}(t) + \tilde{f}(t) \tag{11}$$

$$\tilde{f}(t) = -l_2\tilde{\delta}(t) + k\tilde{f}(t-T) + g(t) \tag{12}$$

where $g(t) = f(t) - kf(t-T)$. Since $|f(t)| \le f_a$, it is clear that $|g(t)| \le (1+k)f_a$. The above error dynamics yields

$$\tilde{\delta}(t)\dot{\tilde{\delta}}(t) = -l_1\tilde{\delta}^2(t) + \tilde{\delta}(t)\tilde{f}(t) \tag{13}$$

$$\begin{aligned} k^2\tilde{f}^2(t-T) =& \tilde{f}^2(t) + l_2^2\tilde{\delta}^2(t) + g^2(t) + 2l_2\tilde{f}(t)\tilde{\delta}(t) \\ & - 2g(t)\tilde{f}(t) - 2l_2g(t)\tilde{\delta}(t). \end{aligned} \tag{14}$$

Theorem 1: Considering the gimbal fault model in (8) with loss of effectiveness fault and additive bias fault. Applying the state observer which is designed as Eq. (9) with iterative fault estimation law in Eq. (10), the gimbal angle estimate error and fault estimate error will ultimately converge to small compact sets containing zero.

Proof: Consider the following Lyapunov function candidate:

$$V = \frac{1}{2}\tilde{\delta}^2(t) + k^2\int_{t-T}^{t}\tilde{f}^2(\nu)d\nu \tag{15}$$

Taking time derivative of V and considering Eqs. (13) and (14), we have

$$\begin{aligned} \dot{V} =& \tilde{\delta}(t)\dot{\tilde{\delta}}(t) + k^2\tilde{f}^2(t) - k^2\tilde{f}^2(t-T) \\ =& \tilde{\delta}(t)\left(-l_1\tilde{\delta}(t) + \tilde{f}(t)\right) + k^2\tilde{f}^2(t) - \tilde{f}^2(t) - l_2^2\tilde{\delta}^2(t) \\ & - g^2(t) - 2l_2\tilde{f}(t)\tilde{\delta}(t) + 2g(t)\tilde{f}(t) + 2l_2g(t)\tilde{\delta}(t) \\ =& -(l_1 + l_2^2)\tilde{\delta}^2(t) - (2l_2 - 1)\tilde{\delta}(t)\tilde{f}(t) - (1-k^2)\tilde{f}^2(t) \\ & - 2l_2\tilde{f}(t)\tilde{\delta}(t) + 2g(t)\tilde{f}(t) + 2l_2g(t)\tilde{\delta}(t) - g^2(t) \end{aligned} \tag{16, 17}$$

Considering the following facts by completion of squares:

$$-(2l_2-1)\tilde{\delta}(t)\tilde{f}(t) \le \frac{2l_2-1}{2}\tilde{\delta}^2(t) + \frac{2l_2-1}{2}\tilde{f}^2(t) \tag{18}$$

$$2g(t)\tilde{f}(t) \le (1+k)f_a + (1+k)f_a\tilde{f}^2(t) \tag{19}$$

$$2l_2g(t)\tilde{\delta}(t) \le (1+k)f_al_2 + (1+k)l_2f_a\tilde{\delta}^2(t), \tag{20}$$

we have

$$\dot{V} \leq -\rho_1 \tilde{\delta}^2(t) - \rho_2 \tilde{f}^2(t) + (1+k)(1+l_2) f_a, \tag{21}$$

where $\rho_1 = l_1 + l_2^2 + \frac{1}{2} - l_2 - (1+k) l_2 f_a$ and $\rho_2 = \frac{3}{2} - k^2 - l_2 - (1+k) f_a$.

If l_1, l_2, and k are selected to satisfy $\rho_1 > 0$ and $\rho_2 > 0$, it is obtained that $\dot{V} < 0$ when

$$|\tilde{\delta}(t)| > \sqrt{\frac{(1+k)(1+l_2) f_a}{\rho_1}}, \tag{22}$$

$$\text{or} \quad |\tilde{f}(t)| > \sqrt{\frac{(1+k)(1+l_2) f_a}{\rho_2}}. \tag{23}$$

This implies that $\tilde{\delta}(t)$ and $\tilde{f}(t)$ are ultimately bounded and converge to compact sets $\mathscr{S}_{\tilde{\delta}}$ and $\mathscr{S}_{\tilde{f}}$, which are respectively defined as

$$\mathscr{S}_{\tilde{\delta}} = \left\{ \tilde{\delta}(t) \,\middle|\, |\tilde{\delta}(t)| \leq \sqrt{\frac{(1+k)(1+l_2) f_a}{\rho_1}} \right\}, \tag{24}$$

$$\mathscr{S}_{\tilde{f}} = \left\{ \tilde{f}(t) \,\middle|\, |\tilde{f}(t)| \leq \sqrt{\frac{(1+k)(1+l_2) f_a}{\rho_2}} \right\}. \tag{25}$$

According to Theorem 1, we can use the developed fault estimation approach to detect and estimate SGCMG gimbal faults in attitude control.

IV. Numerical Simulation

To verify the effectiveness of the proposed fault identification method, numerical simulations under different types of gimbal faults are given.

TABLE II

SIMULATION PARAMETERS

Parameter	value
Mass (kg)	79
Size (mm)	575×572×384
Moment of inertia (kg·m^2)	$\boldsymbol{J}_1 = 3.34$, $\boldsymbol{J}_2 = 5.29$, $\boldsymbol{J}_3 = 3.21$
Slew capacity (deg/s)	$\lvert\omega_1\rvert_{\max} = 8.8$, $\lvert\omega_2\rvert_{\max} = 5.5$, $\lvert\omega_3\rvert_{\max} = 9.1$
Initial attitude	$\boldsymbol{Q}(0) = [0 \quad 0 \quad 0 \quad 1]^T$
Initial rate (deg/s)	$\boldsymbol{\omega}(0) = [0 \quad 0 \quad 0]^T$

TABLE III

SGCMG PARAMETERS

Parameter	value
Skew angle (deg)	54.74
Maximum momentum (Nms)	$h_{\max} = 1$
Maximum output torque (Nm)	$\tau_{\max} = 1$
Maximum gimbal rate (deg/s)	$\dot{\delta}_{\max} = 20$

A. Simulation Specifications

Table II contains the satellite parameters used for the simulations. Four SGCMGs in a regular pyramid configuration are used in simulation. The specification of SGCMG is shown in Table III.

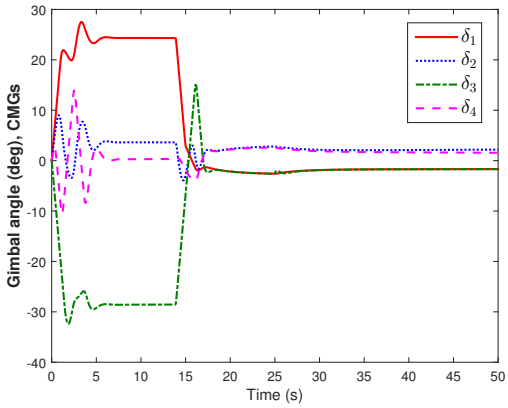

Fig. 4. CMG gimbal angle

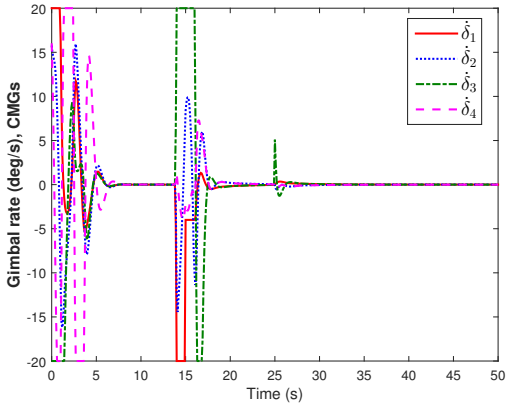

Fig. 5. CMG gimbal rate

The initial condition for satellite is chosen to be $\boldsymbol{Q}(0) = [0,0,0,1]^T$ and $\boldsymbol{\omega}(0) = [0,0,0]^T$ rad/s. The spacecraft is required to perform a single-axis attitude maneuver with 120 deg rotation in roll axis. For the attitude control, the cascade-proportional derivative (PD) attitude controller [19] is employed to accomplish three-axis attitude maneuvers. The parameters in the cascade-PD attitude controller are selected as $k = 17.22$ and $c = 7.55$. Focusing on four SGCMGs, initial gimbal angles are set to $\boldsymbol{\delta}(0) = [0 \quad 0 \quad 0 \quad 0]^T$ deg, which are far away from singular states. We use the singularity escape/avoidance steering law [20] to change the gimbal rate, so that the commanded gimbal rate can be achieved. The parameters in singularity escape/avoidance steering law are selected as:

$$\lambda_0 = 0.01, \quad \mu = 10, \quad \phi_1 = 0, \quad \phi_2 = \frac{\pi}{2}, \quad \phi_3 = \pi,$$
$$\varepsilon_i = 0.01 \sin(0.5\pi t + \phi_i), \quad i = 1,2,3.$$

In the simulation, we assume that the SGCMG 1 experiences 80% loss of its gimbal rate command in 15 seconds and SGCMG 3 encounters 0.1 deg/s bias gimbal rate in 25 seconds. The reason for choosing the two time instances is that the satellite is reorienting and it is easier for us to obverse the fault influences to the attitude maneuver. As for the fault

magnitude, the effectiveness gain under the SGCMG fault is $e_1 = 0.2$, which means that the CMG can only supply 20 percents of its normal output. In this case, a severe loss of effectiveness fault occurs in the SGCMG. If the proposed fault-tolerant attitude control system can handle these severe situations, it of course can deal with the less-severe or minor SGCMG faults.

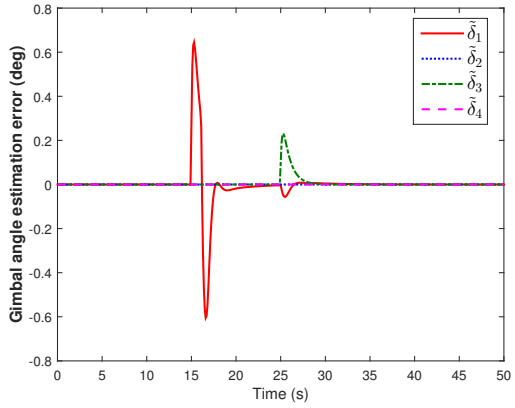

Fig. 6. Gimbal angle estimation error

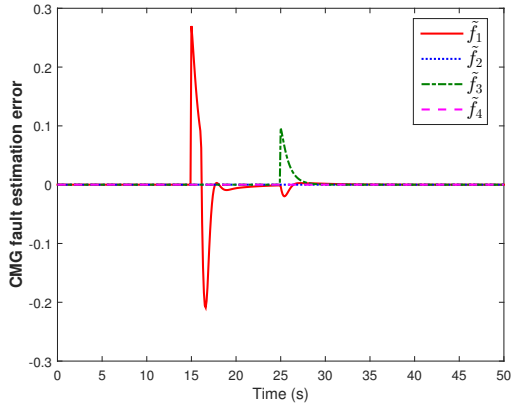

Fig. 7. Fault estimation error

B. Simulation Results

The simulation results under actuator faults are shown in Figs. 4-7. The responses of CMG gimbal angle and gimbal rate under SGCMG fault are illustrated in Figs. 4-5, from which it is clear that the fault affects the responses of gimbal angle and rate. Moreover, it is observed from Figs. 6-7 that the total fault effect of each SGCMG can be estimated accurately using the propose fault estimation method. The estimate process takes around 5 seconds to converge to the estimate errors.

V. Conclusions

In this paper, we develop the mathematical model for SGCMG fault and propose a fault estimation approach to estimate the total fault effects in each SGCMG. Firstly, we consider the SGCMG as a combination of two independent EM-VSD systems, which describe the rotor control loop and gimbal control loop, respectively. For the EM-VSD system, we analyze the potential faults and model them as multiplicative fault and additive fault. Then, we consider two EM-VSD systems together and obtain the SGCMG fault model. To have a simple fault estimation for each SGCMG, the total fault effects are estimated in place of each individual fault. The proposed fault estimation approach is able to exponentially converge the fault estimation error with satisfactory accuracy. Finally, the effectiveness of the proposed SGCMG fault estimation approach is demonstrated by numerical simulations.

References

[1] Y. M. Zhang and J. Jiang, "Bibliographical review on reconfigurable fault-tolerant control systems," *Annual Reviews in Control*, vol. 32, no. 2, pp. 229–252, Dec. 2008.

[2] X. Yu, Y. Fu, P. Li, and Z. Youmin, "Fault-tolerant aircraft control based on self-constructing fuzzy neural networks and multivariable smc under actuator faults," *IEEE Transactions on Fuzzy Systems*, 2018, available online.

[3] X. Yu, P. Li, and Z. Youmin, "The design of fixed-time observer and finite-time fault-tolerant control for hypersonic gliding vehicles," *IEEE Transactions on Industrial Electronics*, vol. 65, no. 5, pp. 4135–4144, 2018.

[4] F. L. Markley and J. L. Crassidis, *Fundamentals of spacecraft attitude determination and control*. Springer, 2014, vol. 33.

[5] S. Murugesan and P. Goel, "Fault-tolerant spacecraft attitude control system," *Sadhana*, vol. 11, no. 1-2, pp. 233–261, 1987.

[6] J. Jiang and X. Yu, "Fault-tolerant control systems: A comparative study between active and passive approaches," *Annual Reviews in control*, vol. 36, no. 1, pp. 60–72, 2012.

[7] A. Noumi and M. Takahashi, "Fault-tolerant attitude control systems for satellite equipped with control moment gyros," in *AIAA Guidance, Navigation, and Control (GNC) Conference*, 2013, AIAA 2013-5119.

[8] A. Fekih, "Fault diagnosis and fault tolerant control design for aerospace systems: A bibliographical review," in *American Control Conference (ACC)*. IEEE, 2014, pp. 1286–1291.

[9] Q. Shen, D. Wang, S. Zhu, and E. K. Poh, "Finite-time fault-tolerant attitude stabilization for spacecraft with actuator saturation," *IEEE Transactions on Aerospace and Electronic Systems*, vol. 51, no. 3, pp. 2390–2405, 2015.

[10] ——, "Robust control allocation for spacecraft attitude tracking under actuator faults," *IEEE Transactions on Control Systems Technology*, vol. 25, no. 3, pp. 1068–1075, 2017.

[11] F. Zhang, L. Jin, and S. Xu, "Fault tolerant attitude control for spacecraft with sgcmgs under actuator partial failure and actuator saturation," *Acta Astronautica*, vol. 132, pp. 303–311, 2017.

[12] Q. Shen, C. Yue, C. H. Goh, B. Wu, and D. Wang, "Rigid-body attitude tracking control under actuator faults and angular velocity constraints," *IEEE/ASME Transactions on Mechatronics*, 2018, available online.

[13] H. A. Toliyat, S. Nandi, S. Choi, and H. Meshgin-Kelk, *Electric Machines: Modeling, Condition Monitoring, and Fault Diagnosis*. CRC Press, 2013.

[14] D. Kastha and B. K. Bose, "Investigation of fault modes of voltage-fed inverter system for induction motor drive," *IEEE Transactions on Industry Applications*, vol. 30, no. 4, pp. 1028–1038, 1994.

[15] S. Nandi, H. A. Toliyat, and X. Li, "Condition monitoring and fault diagnosis of electrical motors — a review," *IEEE transactions on energy conversion*, vol. 20, no. 4, pp. 719–729, 2005.

[16] D. Campos-Delgado, D. Espinoza-Trejo, and E. Palacios, "Fault-tolerant control in variable speed drives: a survey," *IET Electric Power Applications*, vol. 2, no. 2, pp. 121–134, 2008.

[17] J. Chen and R. J. Patton, *Robust model-based fault diagnosis for dynamic systems*. Springer Science & Business Media, 2012, vol. 3.

[18] C. Yue, Q. Shen, C. H. Goh, X. Cao, and T. H. Lee, "A general fault-frame of momentum exchange devices," *IEEE Transactions on Aerospace and Electronic Systems*, 2017, submitted.

[19] B. Wie, *Space Vehicle Dynamics and Control*. AIAA, 2002.

[20] B. Wie, D. Bailey, and C. Heiberg, "Singularity robust steering logic for redundant single-gimbal control moment gyros," *Journal of Guidance, Control, and Dynamics*, vol. 24, no. 5, pp. 865–872, 2001.